

## Synthesis and Enhanced H<sub>2</sub> Adsorption Properties of a Mesoporous Nanocrystal of MOF-5: Controlling Nano-/Mesostructures of MOFs To Improve Their H<sub>2</sub> Heat of Adsorption

Zhifeng Xin,<sup>[a]</sup> Junfeng Bai,<sup>\*[a]</sup> Yi Pan,<sup>[a]</sup> and Michael J. Zaworotko<sup>[b]</sup>

The development of hydrogen as a clean energy source is heavily dependent on its safe and efficient transport and storage.<sup>[1]</sup> Very recently, microporous metal–organic frameworks (MOFs) have been explored intensively as potential hydrogen storage materials<sup>[2]</sup> due to the higher surface areas, higher micropore volumes, and lower density.<sup>[3]</sup> However, hydrogen storage of MOFs requires either high pressure or very low temperature, or both. Moreover, effective hydrogen storage at ambient temperature and lower pressure requires a large improvement in the H<sub>2</sub> heat of adsorption for MOFs.<sup>[4]</sup> Many groups such as those run by Hupp,<sup>[5a–c]</sup> Snurr,<sup>[5d]</sup> Mirkin,<sup>[5e]</sup> Chen,<sup>[5f]</sup> Kaskel,<sup>[5g]</sup> Long,<sup>[5h–j]</sup> and Zhou<sup>[5k]</sup> have effectively improved the H<sub>2</sub> heat of adsorption by cation doping, catenation, increasing the number of unsaturated metal sites, and minimizing the size of micropores.

MOF-5 as an excellent model of this family has been widely investigated because of its thermal stability, high surface area, and excellent hydrogen storage capacity (maximum hydrogen uptake, 76 mg g<sup>-1</sup>).<sup>[6]</sup> Meanwhile, the investigation of nano-/mesostructures of MOFs is still in its infancy.<sup>[7]</sup> Unlike their bulk counterparts, these structures exhibit properties that are often a function of their nano- and microscale architectures.<sup>[7a,b]</sup> Most interestingly, these nano-/mesostructures may create more unsaturated metal sites on the internal or external surface of particles and improve the H<sub>2</sub> heat of adsorption of MOFs. To the best of our knowledge, such work has not been reported. Our group's work is

focused upon the construction and morphologically controllable synthesis of coordination polymers with interesting properties.<sup>[8]</sup> Herein, we report a mesoporous nanocube of MOF-5 (MNMOF-5) with improved H<sub>2</sub> heat of adsorption and also higher H<sub>2</sub>, CO<sub>2</sub>, and CH<sub>4</sub> uptakes at room temperature compared to those of bulky MOF-5 crystals.<sup>[2d, 4b, 6c]</sup>

MNMOF-5 was successfully prepared by diluting the concentration of the reactants by 400 times that reported in the literature for the reaction under solvothermal conditions.<sup>[6a]</sup> The PXRD pattern (see Figure S1 in the Supporting Information) is in accordance with the simulated XRD pattern of MOF-5. MNMOF-5 is stable at 400–500 °C (see Figure S2 in the Supporting Information), which is similar to that of bulky MOF-5 crystals. The SEM images (Figure 1a, b) of MNMOF-5 show that the size of the cube with mesopores on the surface is about 300–400 nm. This mesoporous structure was also observed in the TEM image (Figure 1c). Furthermore, the HRTEM image (Figure 1d) gives the fine nanostructure of MNMOF-5, which is formed by MOF-5 nanocrystals with a diameter of 5–10 nm. The crystal lattice

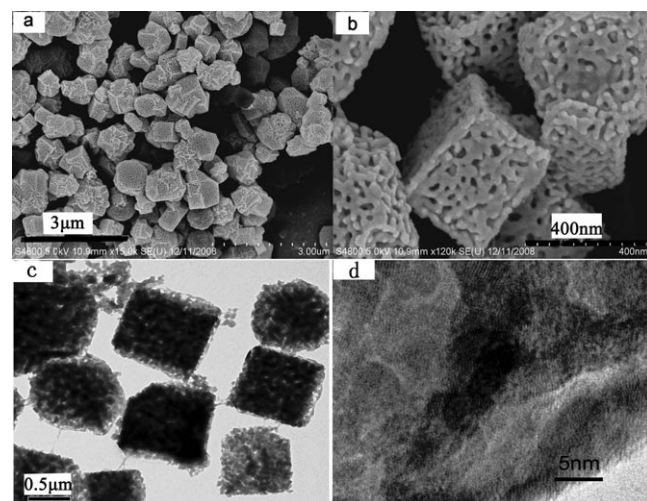


Figure 1. a) FESEM image; b) magnified FESEM image; c) TEM image; and d) HRTEM image of MNMOF-5.

[a] Dr. Z. Xin, Prof. J. Bai, Prof. Y. Pan

Department State Key Laboratory of Coordination Chemistry  
School of Chemistry and Chemical Engineering  
Nanjing University, Nanjing 210093 (China)  
Fax: (+86)25-83593384  
E-mail: bjunfeng@nju.edu.cn

[b] Prof. M. J. Zaworotko

Department of Chemistry, University of South Florida  
CHE205, 4202 East Fowler Avenue  
Tampa, FL, 33620 (USA)

Supporting information for this article is available on the WWW under <http://dx.doi.org/10.1002/chem.201001700>.

of each nanocrystal can be seen in the HRTEM image, and the mesopores are the spaces between these nanocrystals. The pore structure of MNMOF-5 was also probed by a low-pressure  $N_2$  adsorption measurement.

The Langmuir surface area of MNMOF-5 is about  $4218 \text{ m}^2 \text{ g}^{-1}$ , which is similar to the reported  $4400 \text{ m}^2 \text{ g}^{-1}$  of bulky MOF-5 crystals;<sup>[6a]</sup> however, the Brunauer–Emmett–Teller (BET) surface area of MNMOF-5 is about  $3243 \text{ m}^2 \text{ g}^{-1}$ , which is  $557 \text{ m}^2 \text{ g}^{-1}$  smaller than the reported  $3800 \text{ m}^2 \text{ g}^{-1}$  of bulky MOF-5 crystals.<sup>[6a]</sup> This difference may be attributed to the small size of particles, which leads to the decrease of micropore volume.<sup>[9]</sup> The  $N_2$  adsorption isotherm (Figure 2) shows two increasing steps before  $0.1 P/P_0$

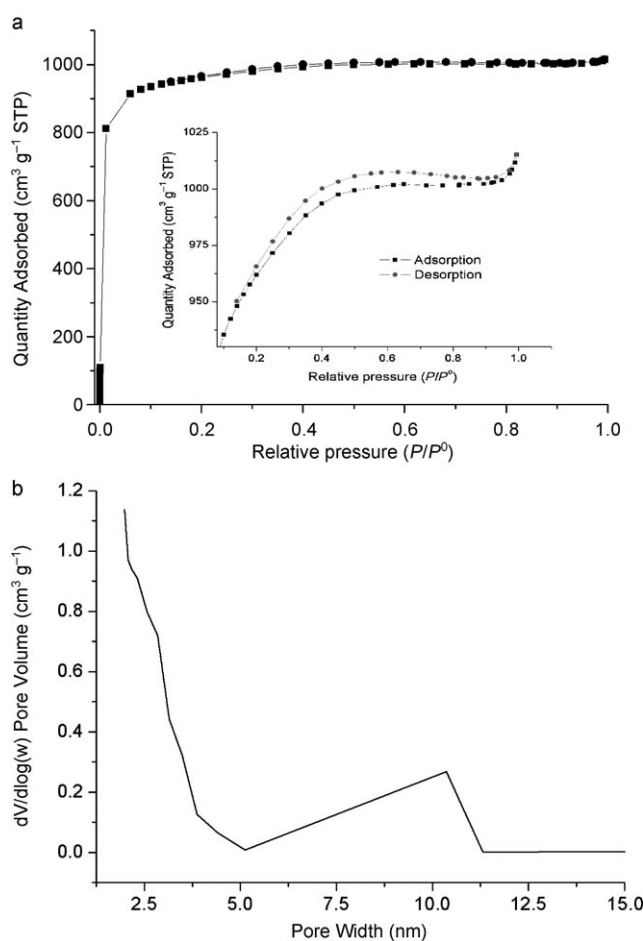


Figure 2. a)  $N_2$  adsorption isotherm of MNMOF-5, the inset is the adsorption isotherm of mesoporous parts in MNMOF-5; b) the mesopore distribution of MNMOF-5.

and before  $0.5 P/P_0$ , which indicate that micro- and mesopores coexist in MNMOF-5. The magnified sorption isotherm of the mesopores part (Figure 2 inset) exhibits a long and sharp hysteresis loop between  $0.2$ – $0.9 P/P_0$ , which reveals the wide mesopore distribution of MNMOF-5 (Figure 2b).

The  $H_2$  isosteric heat of adsorption (Figure 3b) was investigated by using virial equations [Eq. (1) and (2)] according

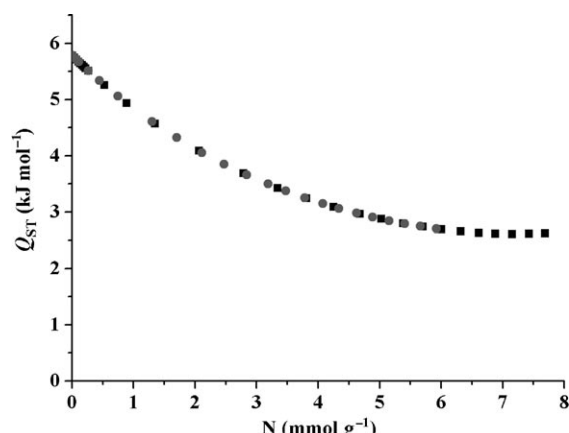


Figure 3. Isosteric  $H_2$  heat of adsorption for MNMOF-5 calculated from the low-pressure  $H_2$  uptakes at  $77 \text{ K}$  (■) and  $87 \text{ K}$  (●).

to the low-pressure  $H_2$  adsorption data at  $77 \text{ K}$  and  $87 \text{ K}$  (see Figure S3a and Figure S4 in the Supporting Information).<sup>[5a]</sup>

$$\ln p = \ln N + \frac{1}{T} \sum_{i=0}^m a_i N^i + \sum_{i=0}^n a_i N^i \quad (1)$$

$$Q_{\text{st}}(N) = -R \sum_{i=1}^m a_i N^i \quad (2)$$

The  $H_2$  heat of adsorption ( $Q_{\text{st}}$ ) for MNMOF-5 is about  $5.78 \text{ kJ mol}^{-1}$ , which, as we anticipated, is increased by about 20% compared to that of MOF-5 reported in reference [4b,c] ( $4.8 \text{ kJ mol}^{-1}$ ). This high  $Q_{\text{st}}$  value at zero coverage may be attributed to the strong physisorption of  $H_2$  onto the unsaturated metal sites on the surface of inter-crystallites mesopores.

High-pressure  $H_2$  uptake was further measured at  $77 \text{ K}$  and  $298 \text{ K}$ .  $H_2$  uptake by MNMOF-5 is about  $64 \text{ mg H}_2 \text{ g}^{-1}$  at  $77 \text{ K}$  and  $20 \text{ bar}$ , however, it did not achieve the isotherm plateau and, therefore, no saturation of  $H_2$  adsorption took place. The  $H_2$  uptake by MNMOF-5 is higher than that of the reported bulky MOF-5 crystals below  $6.5 \text{ bar}$ , but lower than that of the reported  $H_2$  uptake by MOF-5 at  $77 \text{ K}$  (Figure 4) above  $6.5 \text{ bar}$ . Interestingly,  $H_2$  uptake by MNMOF-5 at room temperature ( $1.5 \text{ mg H}_2 \text{ g}^{-1}$  at  $19 \text{ bar}$ ) increases considerably compared with the reported value of bulky MOF-5 crystals ( $1.3 \text{ mg H}_2 \text{ g}^{-1}$  at  $19.7 \text{ bar}$ )<sup>[6a]</sup> (Figure 4 inset). It can be concluded that the higher  $H_2$  heat of adsorption can facilitate the  $H_2$  adsorption at lower pressure or higher temperature.<sup>[2c,3a]</sup> Meanwhile,  $\text{CO}_2$  and  $\text{CH}_4$  uptake by MNMOF-5 is about  $882 \text{ mg g}^{-1}$  (see Figure S5 in the Supporting Information) and  $92 \text{ mg g}^{-1}$ , respectively, (see Figure S6 in the Supporting Information) at  $298 \text{ K}$  and  $20 \text{ bar}$ , which is respectively about 5% and 10% higher than that of MOF-5 bulky crystal (Table 1) under the same conditions.<sup>[4b,6d]</sup>

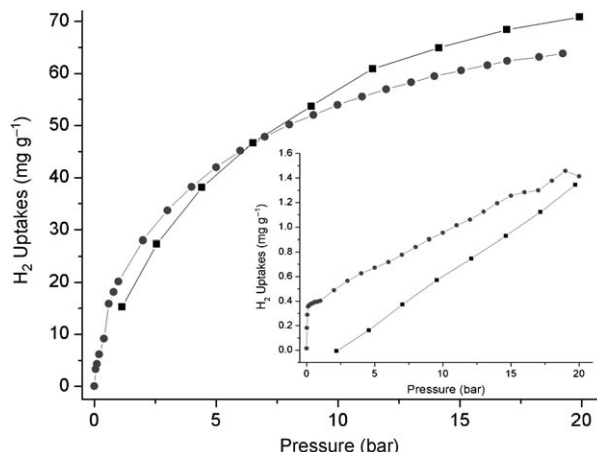


Figure 4. High-pressure H<sub>2</sub> uptake of MNMOF-5 (●) and early reported H<sub>2</sub> uptake of MOF-5 bulky crystals<sup>[6a]</sup> (■) at 77 K and 298 K (inset).

Table 1. Sorption data for MNMOF-5.

| Samples | SA <sub>BET</sub> <sup>[a]</sup><br>[m <sup>2</sup> g <sup>-1</sup> ] | H <sub>2</sub> uptake <sup>[b]</sup><br>[mg g <sup>-1</sup> ] | Q <sub>st</sub> of H <sub>2</sub><br>[kJ mol <sup>-1</sup> ] | CO <sub>2</sub> uptake <sup>[c]</sup><br>[mg g <sup>-1</sup> ] | CH <sub>4</sub> uptake <sup>[c]</sup><br>[mg g <sup>-1</sup> ] |
|---------|---|---|--|--|--|
| MNMOF-5 | 3243  | 64  | 5.87   | 882  | 92   |
| MOF-5   | 3800 <sup>[6a]</sup>  | 7.1 <sup>[6a]</sup>   | 4.8 <sup>[4b,c]</sup>  | 837 <sup>[6d]</sup>  | 82 <sup>[4b]</sup>   |

[a] SA<sub>BET</sub>=Brunauer–Emmett–Teller surface area. [b] H<sub>2</sub> uptake was measured at 77 K. [c] CO<sub>2</sub> and CH<sub>4</sub> uptakes were measured at 298 K. All the gases uptakes were obtained at 20 bar.

In summary, for the first time, a novel mesoporous nanocube of MOF-5 (MNMOF-5) was prepared under solvothermal conditions by diluting the concentration of reactants. Compared to the bulky MOF-5 crystals, our sample includes additional mesoporous structure, and the H<sub>2</sub> heat of adsorption was considerably improved, as were the H<sub>2</sub>, CO<sub>2</sub>, and CH<sub>4</sub> uptakes at room temperature. Moreover, our work shows that controlling nano-/mesostructures of MOFs can improve their H<sub>2</sub> adsorption properties and facilitate the future applications of MOFs.

## Experimental Section

**Materials:** 1,4-Benzenedicarboxylic acid (H<sub>2</sub>BDC) was purchased from Alfa Aesar. Zn(NO<sub>3</sub>)<sub>2</sub>·6H<sub>2</sub>O and N,N'-dimethylformamide (DMF) were purchased from Nanjing Chemical Company.

**Synthesis of the mesoporous nanocube of MOF-5 (MNMOF-5):** H<sub>2</sub>BDC (0.018 g) and Zn(NO<sub>3</sub>)<sub>2</sub>·6H<sub>2</sub>O (0.1 g) were dissolved in a 1800 mL beaker containing DMF (1000 mL). After vigorous stirring for 10 min, the solution was transferred evenly into 15 100 mL Teflon-lined stainless steel autoclaves, sealed, and maintained at 100°C for 7 h. This gave mesoporous microcubic MOF-5 (MNMOF-5). The precipitate was collected and washed with DMF and exchanged with CHCl<sub>3</sub> three times in three days. The material was evacuated at 130°C for 10 h to give a 4283 m<sup>2</sup> g<sup>-1</sup> sample.

**Characterization:** Powder X-ray diffraction (XRD) patterns were collected on a Shimadzu XRD-6000 (operating at 40 kV and 30 mA) with CuK<sub>α</sub> radiation (wavelength  $\lambda=1.5147\text{ \AA}$ ). The thermogravimetric analysis was carried out in flowing N<sub>2</sub> (flow rate: 50 mL min<sup>-1</sup>) with a heating rate of 10°C min<sup>-1</sup> using a STA 449 C DSC-TGA instrument. SEM images were

obtained on a Hitachi S-4800 field emission scanning electron microscope. Transmission electron microscopy (TEM) was performed on a Philips TECNAI F20 S-TWIN TEM instrument using an accelerating voltage of 120 kV, and HRTEM investigations were carried out on a JEOL JEM-2101 electron microscope operating at 200 kV. Nitrogen adsorption and desorption isotherms were measured at 77 K using a Micromeritics ASAP 2020M+C system after the samples were first degassed at 130°C for 10 h. Surface areas were determined by using the BET and Langmuir methods, and the mesopore size distribution was determined by the Barrett–Joyner–Halenda (BJH) method, using the adsorption branch of the isotherm. The mesopore volume ( $V_{\text{meso}}$ ) was obtained from the BJH adsorption cumulative volume of pores between 1.70 nm and 300.00 nm diameter, and the corresponding micropore volume ( $V_{\text{micro}}$ ) was calculated by subtracting the mesopore volume from the total pore volume. The mesopore size was estimated from the maximum point of the BJH pore size distribution plot. The high-pressure H<sub>2</sub> adsorption measurement was recorded at 0–20 bar by using an Intelligent Gravimetric Analysis instrument (IGA-100, Hiden).

## Acknowledgements

The authors gratefully acknowledge supports from the Major State Basic Research Development Programs (Nos. 2006CB806104 and 2007CB936302), the NSFC (Nos. 20771058 and 20931004), and the Science Foundation of Innovative Research Team of the NSFC (No. 20721002).

**Keywords:** hydrogen storage • mesoporous materials • metal–organic frameworks • nanoparticles

- [1] L. Schlapbach, A. Zuttel, *Nature* **2001**, *414*, 353–358.
- [2] a) D. J. Collins, H.-C. Zhou, *J. Mater. Chem.* **2007**, *17*, 3154–3160; b) L. J. Murray, M. Dinca, J. R. Long, *Chem. Soc. Rev.* **2009**, *38*, 1294–1314; c) D. Zhao, D. Yuan, H.-C. Zhou, *Energy Environ. Sci.* **2008**, *1*, 222–235.
- [3] a) H. Furukawa, M. A. Miller, O. M. Yaghi, *J. Mater. Chem.* **2007**, *17*, 3197–3204; b) A. G. Wong-Foy, A. J. Matzger, O. M. Yaghi, *J. Am. Chem. Soc.* **2006**, *128*, 3494–3495; c) J. L. C. Rowsell, A. R. Millward, K. S. Park, O. M. Yaghi, *J. Am. Chem. Soc.* **2004**, *126*, 5666–5667; d) K. L. Lim, H. Kazemian, Z. Yaakob, W. R. W. Daud, *Chem. Eng. Technol.* **2010**, *33*, 213–226.
- [4] a) R. C. Lochan, M. Head-Gordon, *Phys. Chem. Chem. Phys.* **2006**, *8*, 1357–1370; b) W. Zhou, H. Wu, M. R. Hartman, T. Yildirim, *J. Phys. Chem. C* **2007**, *111*, 16131–16137; c) J. L. C. Rowsell, O. M. Yaghi, *J. Am. Chem. Soc.* **2006**, *128*, 1304–1315.
- [5] a) K. L. Mulfort, J. T. Hupp, *Inorg. Chem.* **2008**, *47*, 7936–7938; b) K. L. Mulfort, J. T. Hupp, *J. Am. Chem. Soc.* **2007**, *129*, 9604–9605; c) K. L. Mulfort, T. M. Wilson, M. R. Wasielewski, J. T. Hupp, *Langmuir* **2009**, *25*, 503–508; d) P. Ryan, L. J. Broadbelt, R. Q. Snurr, *Chem. Commun.* **2008**, 4132–4134; e) Y.-M. Jeon, G. S. Armatas, J. Heo, M. G. Kanatzidis, C. A. Mirkin, *Adv. Mater.* **2008**, *20*, 2105–2110; f) B. Chen, N. W. Ockwig, A. R. Millward, D. S. Contreras, O. M. Yaghi, *Angew. Chem.* **2005**, *117*, 4823–4827; *Angew. Chem. Int. Ed.* **2005**, *44*, 4745–4749; g) M. Sabo, A. Henschel, H. Fröde, E. Klemmb, S. J. Kaskel, *J. Mater. Chem.* **2007**, *17*, 3827–3832; h) M. Dinca, J. R. Long, *J. Am. Chem. Soc.* **2007**, *129*, 11172–11176; i) M. Dinca, J. R. Long, *Angew. Chem.* **2008**, *120*, 6870–6884; *Angew. Chem. Int. Ed.* **2008**, *47*, 6766–6779; j) M. Dinca, A. Dailly, C. Tsay, J. R. Long, *Inorg. Chem.* **2008**, *47*, 11–13; k) S. Ma, J. Eckert, P. M. Forster, J. Yoon, Y. Hwang, J.-S. Chang, C. D. Collier, J. B. Parise, H.-C. Zhou, *J. Am. Chem. Soc.* **2008**, *130*, 15896–15902.

- [6] a) S. S. Kaye, A. Dailly, O. M. Yaghi, J. R. Long, *J. Am. Chem. Soc.* **2007**, *129*, 14176–14177; b) H. Li, M. Eddaoudi, M. O’Keeffe, O. M. Yaghi, *Nature* **1999**, *402*, 276–279; c) H. Furukawa, O. M. Yaghi, *J. Am. Chem. Soc.* **2009**, *131*, 8875–8883; d) A. R. Millward, O. M. Yaghi, *J. Am. Chem. Soc.* **2005**, *127*, 17998–17999.
- [7] a) A. M. Spokoyny, D. Kim, A. Sumrein, C. A. Mirkin, *Chem. Soc. Rev.* **2009**, *38*, 1218–1227; b) W. Lin, W. J. Rieter, K. M. L. Taylor, *Angew. Chem.* **2009**, *121*, 660–668; *Angew. Chem. Int. Ed.* **2009**, *48*, 650–658; c) L. Qiu, T. Xu, Z. Li, Y. Wu, X. Jiang, L. Zhang, *Angew. Chem.* **2008**, *120*, 9629; *Angew. Chem. Int. Ed.* **2008**, *47*, 9487–9491; d) Y-M. Jeon, G. S. Armatas, D. Kim, M. G. Kanatzidis, C. A. Mirkin, *Small* **2009**, *5*, 46–50; e) Z. Xin, J. Bai, Y. Shen, Y. Pan, *Cryst. Growth Des.* **2010**, *10*, 2451–2454.
- [8] a) S. Wang, H. Xing, Y. Li, J. Bai, M. Scheer, Y. Pan, *Chem. Commun.* **2007**, 2293–2295; b) S. Wang, H. Xing, Y. Li, J. Bai, M. Scheer, Y. Pan, *Chem. Commun.* **2007**, 4416–4418; c) J. Bai, A. V. Virovets, M. Scheer, *Science* **2003**, *300*, 781–783; d) B. Zheng, H. Dong, J. Bai, Y. Li, S. Li, M. Scheer, *J. Am. Chem. Soc.* **2008**, *130*, 7778–7779; e) L. Chen, Y. Shen, J. Bai, C. Wang, *J. Solid State Chem.* **2009**, *182*, 2298–2306.
- [9] a) C.-Y. Hsu, A. S. T. Chiang, R. Selvin, R. W. Thompson, *J. Phys. Chem. B* **2005**, *109*, 18804–18814; b) J. Aguado, D. P. Serrano, J. M. Escola, J. M. Rodríguez, *Micropor. Mesopor. Mater.* **2004**, *75*, 41–49; c) J. Cravillon, S. Münzer, S.-J. Lohmeier, A. Feldhoff, K. Huber, M. Wiebecke, *Chem. Mater.* **2009**, *21*, 1410–1412.

Received: June 16, 2010

Published online: October 13, 2010